Bioorganic & Medicinal Chemistry 18 (2010) 3169–3174

Contents lists available at ScienceDirect

Bioorganic & Medicinal Chemistry

journal homepage: www.elsevier.com/locate/bmc

Anti-microtubule 'plinabulin' chemical probe KPU-244-B3 labeled both α- and β-tubulin

Yuri Yamazaki [a], Makiko Sumikura [b], Koushi Hidaka [b], Hiroyuki Yasui [c], Yoshiaki Kiso [b], Fumika Yakushiji [a], Yoshio Hayashi [a,*]

[a] Department of Medicinal Chemistry, Tokyo University of Pharmacy and Life Sciences, Hachioji, Tokyo 192-0392, Japan
[b] Department of Medicinal Chemistry, Center for Frontier Research in Medicinal Science, Kyoto Pharmaceutical University, Kyoto 607-8412, Japan
[c] Department of Analytical and Bioinorganic Chemistry, Kyoto Pharmaceutical University, Kyoto 607-8414, Japan

ARTICLE INFO

Article history:
Received 30 January 2010
Revised 13 March 2010
Accepted 16 March 2010
Available online 23 March 2010

Keywords:
Anti-cancer agent
Diketopiperazine
Phenylahistin
Tubulin
Vascular disrupting agent

ABSTRACT

Plinabulin (**1**, NPI-2358), a potent microtubule-targeting agent derived from the natural diketopiperazine 'phenylahistin' with a colchicine-like tubulin depolymerization activity, is an anticancer agent undergoing Phase II clinical trials in four countries including the United States. In order to understand the precise binding mode of plinabulin with tubulin, a new bioactive biotin-tagged photoaffinity probe **4** (KPU-244-B3) was designed and synthesized. Probe **4** showed significant binding affinity to tubulin in a binding assay, and selectively bound to tubulin in an HT-1080 cell lysate without photo-irradiation. In a tubulin photoaffinity labeling study, probe **4** labeled both α- and β-tubulin subunits and these interactions were competitively inhibited by plinabulin during photo-irradiation. These results suggest that plinabulin binds in the boundary region between α- and β-tubulin near the colchicine binding site, and not inside the colchicine binding cavity.

1. Introduction

Microtubules are noncovalent polymers of the protein tubulin that are found in all dividing eukaryotic cells and in most differentiated cell types.[1] This cytoskeletal system of eukaryotic cells is an attractive target for the development of anticancer chemotherapeutic agents.[2,3] Chemicals that target microtubules disrupt and suppress the function by inhibiting or promoting microtubule assembly.[3] These actions result in cell cycle arrest in the mitotic phase. Taxoids, which promote microtubule assembly, and *vinca* alkaloids, which inhibit microtubule polymerization, are clinically used anticancer microtubule-targeting agents.[3–6] Colchicine is another important microtubule-targeting agent, which recognizes the colchicine binding site, leading to the inhibition of microtubule polymerization. Although colchicine has limited medical application due to its high toxicity, colchicine has played a fundamental role in elucidating the properties and functions of tubulins and microtubules.[3] Many natural products that recognize the colchicine binding site have been reported such as podophyllotoxin, steganacin, combretastatin, and the flavonoids.[7,8] These compounds share common structural features including a biaryl system tethered by a hydrocarbon linker of variable length.

Over the years, our research has focused on another natural colchicine-like tubulin depolymerization agent 'phenylahistin' (PLH, halimide).[9–12] PLH has a distinctive structure that includes a relatively hydrophilic diketopiperazine (DKP) skeleton. Through the synthesis of a number of derivatives of phenylahistin, we developed plinabulin (NPI-2358/KPU-2, **1**, IC_{50} of 15 nM against HT-29 cells, Fig. 1), a highly potent microtubule depolymerization agent with a didehydroDKP structure. Plinabulin is being evaluated as an anticancer drug in Phase II clinical trials in four countries including the United States. Plinabulin was also recently shown to function as a strong 'vascular disrupting agent' (VDA) to induce tumor-selective vascular collapse.[13–15]

Although PLH is known to competitively inhibit the binding of colchicine to tubulin,[10] the precise binding mode and microtubule depolymerization mechanism of our didehydroDKP-type inhibitors, for example, plinabulin, have not been well investigated. Further, plinabulin and colchicine are not well superimposed in computer-assisted molecular modeling.[16] In a previous study, we synthesized two biologically active photoaffinity probes with a biotin-tag based on the chemical structure of a potent derivative KPU-244 (**2**, IC_{50} of 4 nM against HT-29 cells, Fig. 1). These probes recognized tubulin probably at or near the colchicine binding site, as demonstrated by the competitive inhibition of photoaffinity labeling in the presence of colchicine.[16] However, the resolution of the photoaffinity labeling using these probes was insufficient to precisely characterize the binding interaction. Specifically,

* Corresponding author. Tel./fax: +81 42 676 3275.
E-mail address: yhayashi@toyaku.ac.jp (Y. Hayashi).

0968-0896/$ - see front matter © 2010 Elsevier Ltd. All rights reserved.
doi:10.1016/j.bmc.2010.03.037

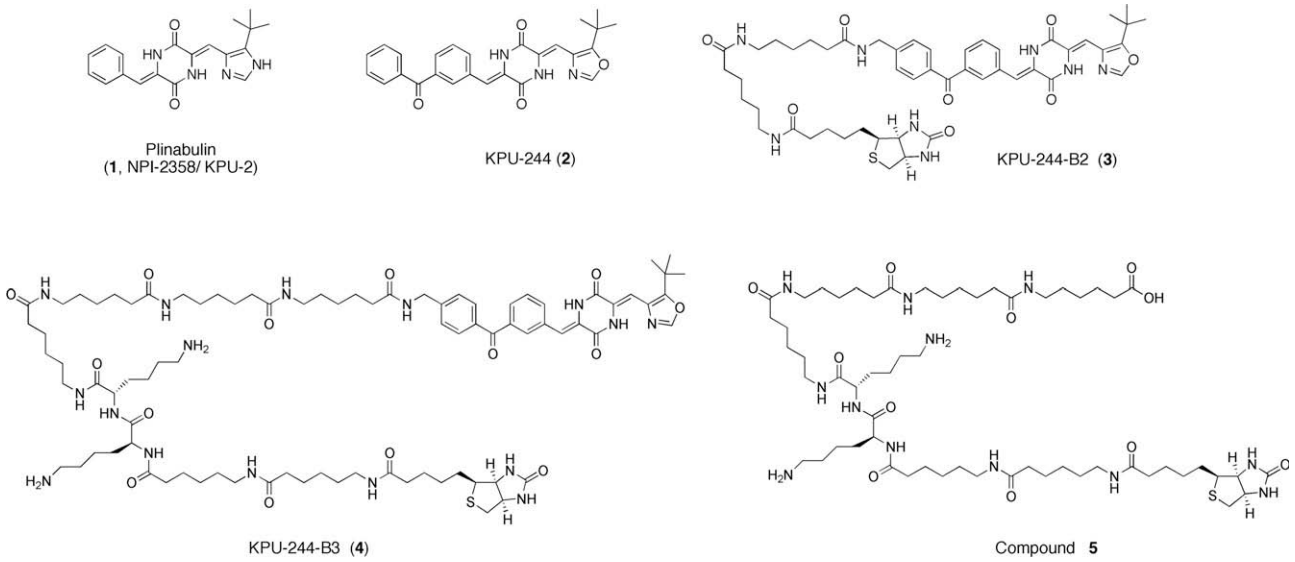

Figure 1. Structures of plinabulin **1** (NPI-2358/KPU-2), KPU-244 **2**, biotin-tagged photoaffinity probes (KPU-244-B2 **3**, KPU-244-B3 **4**), and control compound **5**.

assigning which subunits (α- or β-tubulin) were photolabeled was difficult. To address the issue of low sensitivity of the chemical probes, we investigated whether a long linker between biotin and a ligand would enhance detection in the biotin-avidin detection system.[17] A new photoaffinity probe **4** (Fig. 1), which has a longer linker than probe **3**, was synthesized and was found to exhibit significant binding to porcine tubulin. To investigate the binding mode of probe **4**, tubulin affinity labeling was performed with or without photo-irradiation. In both cases, selective affinity labeling of probe **4** was observed at the α- and β-tubulin subunits.

2. Results and discussion

2.1. Chemistry

Photoaffinity probe **4** was synthesized in a similar manner as that previously described for probe **3**.[16] Briefly, Boc-protected biotinyl peptide **7** (biotinyl-Acp-Acp-Lys(Boc)-Lys(Boc)-Acp-Acp-Acp-Acp-OH, Acp: aminocaproyl), which was accessed from standard Fmoc-based solid phase chemistry (Supplementary data, Scheme S1), was coupled to compound **6**[16] by using EDC–HOBt coupling conditions (Scheme 1). After deprotection of the Boc groups on the linker unit with 4 M HCl in dioxane, the crude product was purified by HPLC to afford the desired compound **4** in 29% yield over two steps. To provide a negative control, compound **5** was synthesized by deprotecting peptide **7** with 50% TFA in CH_2Cl_2 followed by purification by preparative HPLC (Supplementary data, Scheme S2).

2.2. Tubulin binding assay

To determine whether synthetic photoaffinity probe **4** has affinity for tubulin, we performed a binding assay with purified porcine

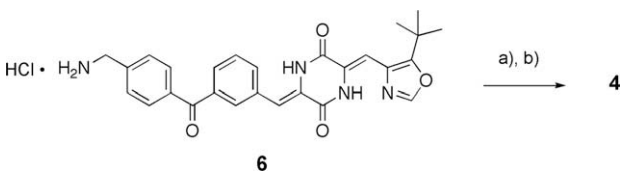

Scheme 1. Synthesis of photoaffinity probe **4**. Reagents and conditions: (a) Boc-protected biotinyl peptide **7**, EDC·HCl, HOBt·H_2O, Et_3N, DMF, rt; (b) 4 M HCl-dioxane, rt, then HPLC purification, 29% over two steps.

tubulin (0.5 μM) in MES buffer (pH 6.8) at 37 °C. The dissociation constants (K_d) of photoaffinity probe **4** and plinabulin **1** were calculated to be 25.17 and 1.06 μM, respectively (Fig. 2 for probe **4** and Fig. S1 for plinabulin **1**). Although the binding affinity of **4** largely decreased from that of **1**, the binding ability of **4** was found to be still significant. Further, the K_d value of **4** was 2.5 times lower than that of photoaffinity probe **3** (K_d = 9.74 ± 2.11 μM against porcine tubulin, Fig. S2), which has a shorter linker and also exhibits mild anti-tubulin polymerization activity and cytotoxicity. This lower K_d value of **4** could be due to the elongation of the biotin linker. We concluded that photoaffinity probe **4** exhibits specific binding to tubulin.

2.3. Affinity binding of probe 4 to tubulin in human cell lysate

We performed a pull-down assay using probe **4** conjugated streptavidin beads from human fibrosarcoma (HT-1080) cell lysate in order to understand the binding affinity of the probe to human tubulin. The whole cell lysate of HT-1080 was incubated with photoaffinity probe **4** conjugated beads at 4 °C overnight, and the proteins retained on the beads were analyzed by Western blots. As shown in Figure 3, α- and β-tubulin were detected as the bound proteins on probe **4** (lane 2), while they were not detected using compound **5** conjugated beads and unconjugated-beads as negative controls (lanes 3 and 4). Moreover, affinity binding of probe **4** to β-actin, which is another major protein of cytoskeleton as tubulin in eukaryotic cells,[18] was not observed (lower panel in Fig. 3). These results suggested that probe **4** selectively bound to human tubulin in the whole cell lysate.

2.4. Tubulin photoaffinity labeling

Upon confirmation of the tubulin binding activity of photoaffinity probe **4**, porcine tubulin was photo-irradiated at 365 nm in the presence of **4** on ice after incubation at 37 °C in MES buffer (containing 1 mM GTP, pH 6.8) for the appropriate duration. The sample was then applied to SDS–PAGE using 7.5% polyacrylamide gels under conditions optimized for separating the α- and β-subunits of tubulin.[19] The protein was stained with Coomassie Brilliant Blue (CBB) or transferred onto a nitro-cellulose membrane, and then an ECL streptavidin-HRP conjugate was used for enzymatic detection. For the SDS–PAGE analysis using CBB staining, neither a remarkable protein band shift nor the appearance of other bands

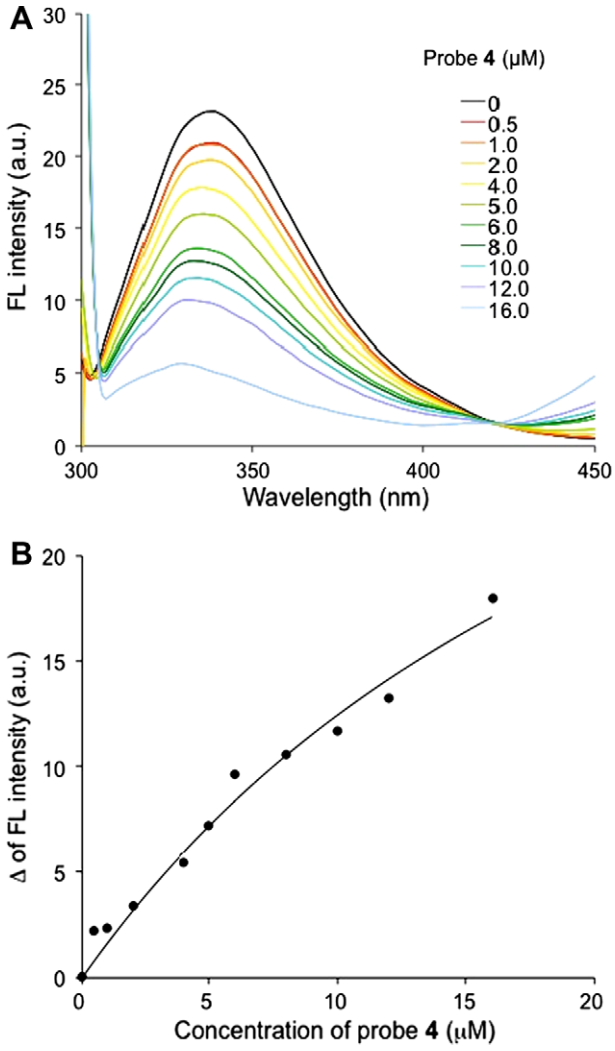

Figure 2. Binding assay based on fluorescence quenching. (A) Effects of probe **4** on tubulin fluorescence. (B) Increase of tubulin photoaffinity probe **4** binding complex. Tubulin (0.5 μM) was incubated in the absence or presence of photoaffinity probe **4** at 37 °C for 1 h. After incubation, the samples were excited at 295 nm, and the emission at 300–450 nm was measured (K_d; the dissociation constant, n; the number of binding sites). K_d and n of photoaffinity probe **4** were 25.17 ± 8.15 μM and 1, respectively.

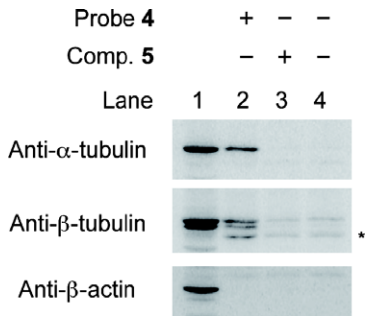

Figure 3. Affinity binding of probes to tubulin in HT-1080. Lane 1: whole cell lysate, lanes 2–4: eluants of protein retained on probe **4** conjugated beads, compound **5** conjugated beads, and unconjugated-beads, respectively. The lower band indicated by an asterisk in the middle panel was suggested a non-specific band.

was observed, indicating that tubulin remained mostly undamaged by photo-irradiation (Fig. 4A, lanes 1 and 2). In addition, non-specific binding was not observed in Western blotting for the non-photo-irradiated sample (Fig. 4A, lane 3). On the other hand, an irradiation-time-dependent labeling was observed in the photo-irradiated samples in the presence of probe **4** (Fig. 4A, lanes 4–6). Probe **4** labeled tubulin as two clearly separated bands, while probe **3**, which has a shorter linker, labeled tubulin as an ambiguous broad band (Fig. 4B, lane 7). These results suggest that probe **4** detects tubulin at a higher resolution than probe **3**. The observed difference in resolution is probably due to the biotin-avidin detection system, in which recognition of biotin is preferable to that of avidin when a long linker is used, whereas the binding affinity (K_d value) of probe **4** was lower than that of probe **3**. To determine which subunits of tubulin were in the observed two bands, immunoblot analysis using α- and β-tubulin specific antibodies was performed after detecting photolabeled protein with a streptavidin-HRP system. The upper and lower bands were found to be derived from α- and β-tubulin, respectively (Fig. 4C, lanes 9 and 10), indicating that photoaffinity probe **4** photolabeled both α- and β-tubulin subunits. In contrast, the binding selectivity of probe **3** could not be determined in a previous study because probe **3** labeled tubulin as a broad band.[16] Furthermore, a competitive photoaffinity labeling study with photoaffinity probe **4** was performed in the absence or presence of plinabulin **1** to elucidate the selectivity of photoaffinity binding. A dose-dependent inhibition of photoaffinity labeling was observed in the presence of plinabulin **1** (Fig. 4D, lanes 12–14), indicating that probe **4** recognizes the same binding site on tubulin as plinabulin. Photoaffinity labeling of tubulin with probe **4** was also inhibited by the addition of excess colchicine (100 equiv, Fig. 4E, lane 16). In addition, the inhibition was specific to colchicine, but not biotin as a negative control in a dose-dependent (5–100 equiv) competitive assay (Supplementary data, Fig. S3). This result is consistent with previous report that PLH, an original compound of plinabulin, competed with [^{3}H]colchicine for tubulin.[10] Therefore, we concluded that probe **4** binds the boundary region between α- and β-tubulin at or near the colchicine binding site.

To examine the precise binding of plinabulin derivatives at the colchicine binding site, a docking study was performed using the molecular modeling package MOE 2008.10 (Chemical Computing Group, Inc., Montreal, Canada). To simplify calculations, a highly potent plinabulin derivative **2** was used in the docking study instead of probe **4**, which contains a long biotin linker. Tubulin proteins (chains A and B) were exploited from crystallographic data in complex with colchicine (PDB ID, 1SA0). Compound **2** was docked around the colchicine binding site on the tubulin dimer and the conformations with high docking scores were chosen. Next, energy minimization and molecular dynamic (MD) simulations were successively performed. The binding interaction in which compound **2** was exclusively inserted into the colchicine binding pocket (Supplementary data, Fig. S4) was examined. Although the photoreactive benzophenone moiety stuck out from the pocket, this reactive part could only recognize the β-subunit at a distance of about 4 Å, which meant that binding to the side chains of Asn249β and Lys254β could occur. However, the reactive benzophenone group could not bind to the α-subunit due to presence in GTP. The benzophenone oxygen was far from the α-subunit with a distance of more than 7 Å. These results suggest that it is difficult to photolabel both subunits in this model. However, when compound **2** was docked on the outside of the colchicine binding pocket, as shown in Figure 5a, it would more likely interact with tubulin in a manner consistent with the experimental results. In this model, compound **2** is located at the interfacial region of the α- and β-subunits, and this region partially overlaps with the colchicine binding pocket. The *tert*-butyl group, which is crucial for the potent biological activity of plinabulin derivatives, covers the colchicine binding pocket. Compound **2** could interact with Ser178α, Tyr210α, Pro222α, Val355β and Gln427β on α- and β-tubulin via four water

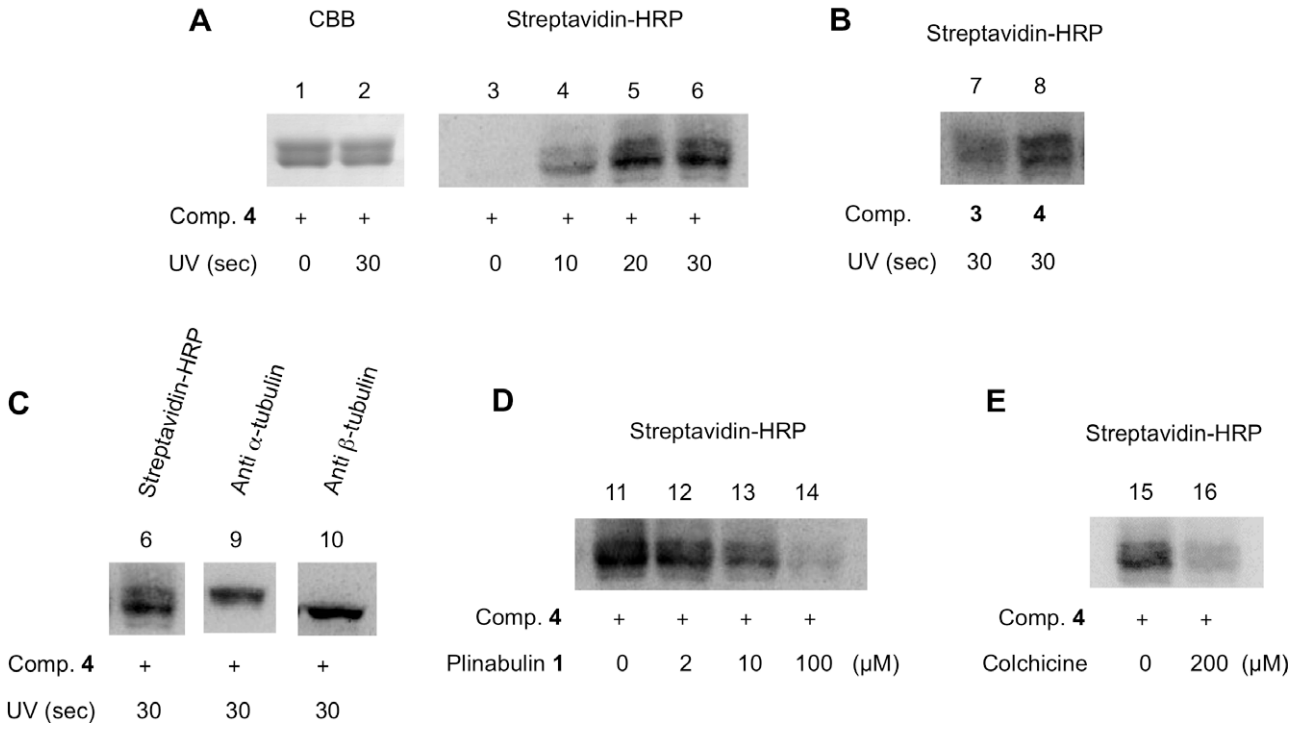

Figure 4. Photoaffinity labeling of tubulin. (A) Photoaffinity labeling by probe **4** at different irradiation times. Porcine tubulin (2 μM) was incubated with probe **4** (2 μM) at 37 °C and then photo-irradiated for the appropriate time (0–30 s). Photolabeled samples were resolved by SDS–PAGE using 7.5% polyacrylamide gels. The gel was analyzed by CBB staining (lanes 1 and 2) or Western blotting followed by enzymatic detection system using ECL streptavidin-HRP conjugate (lanes 3–6). (B) Comparison of tubulin photoaffinity labeling between photoaffinity probe **3** (lane 7) and **4** (lane 8). Tubulin incubated at 37 °C with probe **3** (2 μM) or **4** (2 μM) was photo-irradiated for 30 s. Western blotting analysis was performed as described in Figure 3A. (C) Immunoblot analysis of photolabeled tubulin using α- and β-tubulin specific antibodies (lanes 9 and 10). (D) Photoaffinity labeling of tubulin with probe **4** (2 μM) in the absence (lane 11) or presence of plinabulin **1** (2–100 μM, lanes 12–14). Samples were photo-irradiated for 30 s. (E) Photoaffinity labeling of tubulin with probe **4** (2 μM) in the absence (lane 15) or presence of colchicine (200 μM, lane 16). Samples were photo-irradiated for 30 s.

molecules (Fig. 5b). For photoaffinity labeling with the benzophenone moiety, there were three accessible C–H bonds, which were on the α-carbon of Thr223α and on the γ- and ε-carbons of Met325β, and the distance between each carbonyl oxygen and hydrogen atom was within 3.3 Å (Fig. 5c). Results from previous studies indicated that the reactive volume of the benzophenone moiety could be approximated as a sphere with a radius of 3.1 Å centered on the oxygen[20] and that benzophenone could selectively interact with Met residues with a photoaffinity labeling radius of 6–7 Å.[21] The modeling study of probe **4**, which contains a biotin long linker extending from the benzophenone moiety, suggested that the linker can stick out from the interfacial region to outside the molecules through a space formed between α- and β-tubulin. In this modeling, the corresponding binding conformation of compound **2** on probe **4** was almost maintained (Supplementary data, Fig. S5). From these reports, the binding model shown in Figure 5 represents a reasonable model for photolabeling both α- and β-subunits. Therefore, plinabulin derivatives interact with the boundary region between α- and β-tubulin around the colchicine binding site, and not inside the colchicine binding site. Considering the findings in this docking study, identifying the amino acid residues that are modified by the photoaffinity probe would be of interest in future studies involving mass spectrometry analysis of the photoaffinity labeling of tubulin. This analysis is currently underway and the results will be reported in due course.

3. Conclusion

We designed and synthesized a new bioactive biotin-tagged photoaffinity probe KPU-244-B3 (**4**) containing a long linker. Photoaffinity probe **4** exhibited significant binding to tubulin in a binding assay using porcine tubulin, and also bound to human tubulin in an HT-1080 lysate. Furthermore, in a photoaffinity labeling study, probe **4** recognized both α- and β-tubulin subunits, and this labeling was inhibited by the addition of plinabulin **1** or colchicine. These results revealed that probe **4** bound in the boundary region between α- and β-tubulin around the colchicine binding site. Molecular modeling studies suggested that plinabulin derivatives could interact in the interfacial region of α- and β-tubulin, which partially overlaps with the colchicine binding site. This hypothesis is supported by the results that both α- and β-subunits were clearly photolabeled by probe **4** in the present study. These findings would help determine the amino acid residues that are modified by the photoaffinity probes, leading to a profound understanding of the tubulin depolymerization activity of plinabulin.

4. Experimental

4.1. General

Reagents and solvents were purchased from Wako Pure Chemical Ind., Ltd (Osaka, Japan), Nakalai Tesque (Kyoto, Japan), and Aldrich Chemical Co. Inc. (Milwaukee, WI) and used without further purification. Porcine tubulin was purchased from Cytoskeleton, Inc. (Denver, Colorado, USA). All other chemicals were of the highest commercially available purity. Analytical thin-layer chromatography (TLC) was performed on Merck Silica Gel $60F_{254}$ precoated plates. Preparative HPLC was performed using a C18 reverse-phase column (19 × 100 mm; SunFire™ Prep C18 OBD™ 5 μm) with a binary solvent system: a linear gradient of CH_3CN in 0.1% aqueous TFA at a flow rate of 10 mL/min, detected at UV 230 nm and 365 nm. Solvents used for HPLC were HPLC-grade solvents. All

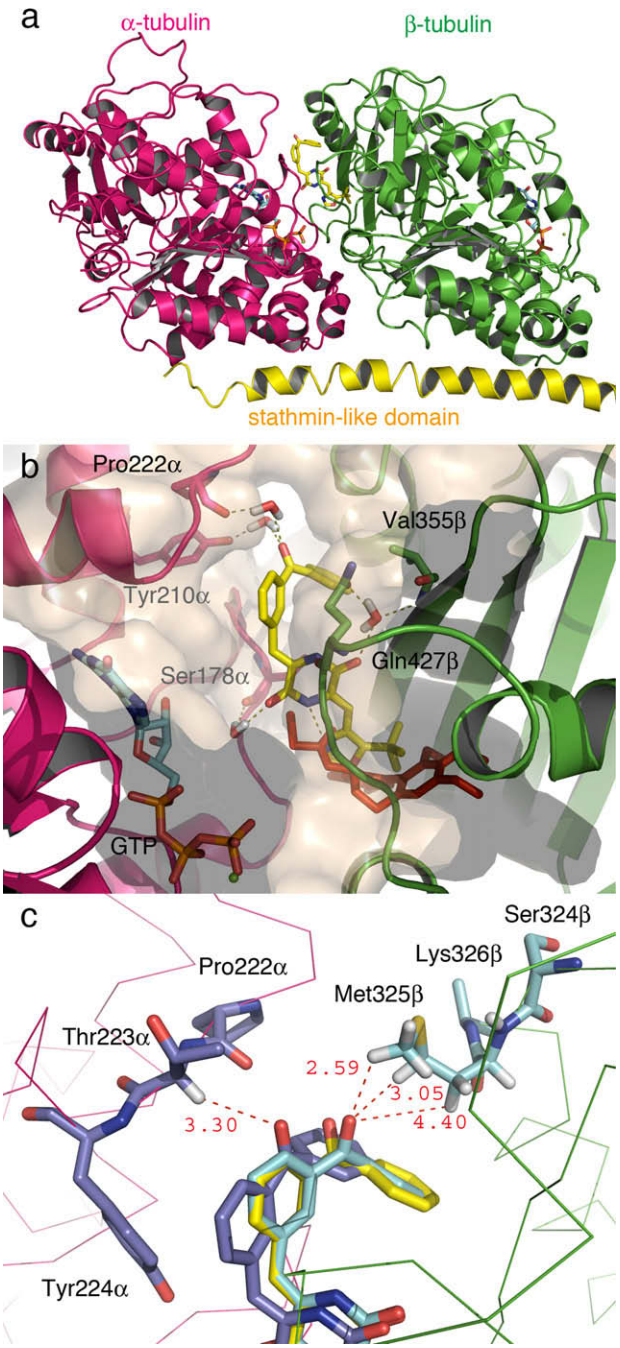

Figure 5. Molecular dynamics simulated poses of compound **2** (yellow stick) in a tubulin heterodimer (magenta and green): (a) full structure; (b) binding area superimposed with colchicine (red stick); (c) the approaching benzophenone carbonyl group poses between the α-chain (blue stick) and β-chain (cyan stick) during the simulation.

other chemicals were of analytical grade or better. Proton (^{1}H) NMR spectra were recorded on a BRUKER AV600 at 600 MHz for proton. Chemical shifts were recorded as δ values in parts per million (ppm) downfield from tetramethylsilane (TMS). High-resolution mass spectra (TOF) were recorded on a micromass Q-Tof Ulitima API.

4.2. Boc-protected biotinyl peptide (biotinyl-Acp-Acp-Lys(Boc)-Lys(Boc)-Acp-Acp-Acp-Acp-OH) (7)

Biotinyl peptide **7** was synthesized by coupling Fmoc-aminohexanoic acid, Fmoc-Lys(Boc)-OH, and D-biotin using conventional Fmoc-based solid phase chemistry on a 2-chlorotrityl chloride resin (1.29 mmol/g).[22] After complete elongation of the peptide chain, Boc-protected peptide **7** was cleaved from the resin by treatment with DCM/AcOH/TFE (7:1:2, TFE, tetrafluoroethanol) for 1 h at room temperature.[23] The reaction mixture was then filtered to remove the resin and the obtained filtrate was concentrated in vacuo, followed by precipitation and centrifugation with Et_2O at 4 °C. The resultant crude biotinyl peptide **7** (431 mg, 66%) was used in the next reaction with no further purification; HRMS (TOF): *m*/*z* 1379.8949 ($M+H^+$) (calcd for $C_{68}H_{123}N_{12}O_{15}S$: 1379.8952).

4.3. KPU-244-B3 (4)

To a solution of peptide **7** (81 mg, 0.058 mmol) in DMF (5 mL) were added sequentially HOBt·H_2O (8 mg, 0.058 mmol), EDC·HCl (12 mg, 0.058 mmol), compound **6** (14 mg, 0.03 mmol; prepared by deprotecting the *N*-Boc-protected derivative of compound **6** (structure not shown)[16] using 4 M HCl in dioxane), and Et_3N (4 μL, 0.03 mmol). The mixture was stirred at room temperature for 20 h. After the solvent was removed in vacuo, the residue was extracted with AcOEt, washed with 10% citric acid, 10% $NaHCO_3$ and saturated NaCl. The organic layer was dried over anhydrous Na_2SO_4 and concentrated in vacuo. The resultant residue was dissolved in 4 M HCl in dioxane (2 mL) and stirred at room temperature for 1 h. After the solvent was removed in vacuo, the residue was purified by preparative HPLC (with a linear gradient of 20–65% CH_3CN in 0.1% aqueous TFA over 40 min) and the collected fractions were lyophilized to give a pale yellow powder (16 mg, 29% over two steps); ^{1}H NMR (600 MHz, DMSO-d_6) δ 1.19–1.38 (m, 30H), 1.40 (s, 9H), 1.43–1.56 (m, 21H), 1.58–1.65 (m, 3H), 2.00–2.05 (m, 10H), 2.08–2.13 (m, 2H), 2.16 (t, 2H, J = 7.4 Hz), 2.58 (d, 1H, J = 12.5 Hz), 2.75–2.77 (m, 4H), 2.82 (dd, 1H, J = 5.1, 12.5 Hz), 2.99–3.06 (m, 12H), 3.08–3.11 (m, 1H), 4.11–4.23 (m, 3H), 4.31 (dd, 1H, J = 5.2, 7.4 Hz), 4.37 (d, 2H, J = 5.8 Hz), 6.38 (s, 1H), 6.43 (s, 1H), 6.72 (s, 1H), 6.86 (s, 1H), 7.43 (d, 2H, J = 8.3 Hz), 7.58 (s, 1H), 7.62–7.64 (m, 6H), 7.71–7.79 (m, 7H), 7.81 (s, 1H), 7.87–7.90 (m, 2H), 7.95 (d, 1H, J = 7.6 Hz), 8.42 (t, 1H, J = 5.9 Hz), 8.61 (s, 1H), 10.59 (s, 1H), 11.13 (s, 1H); HRMS (TOF): *m*/*z* 1631.9712 ($M+H^+$) (calcd for $C_{85}H_{131}N_{16}O_{14}S$: 1631.9751).

4.4. Compound 5

For Boc-deprotection, crude peptide **7** (20 mg) was dissolved in 50% TFA/CH_2Cl_2 (v/v, 2 mL), and stirred at room temperature for 30 min. After the solvent was removed by evaporation, dry ether was added and the resulting powder was purified by preparative HPLC (with a linear gradient of 15–40% CH_3CN in 0.1% aqueous TFA over 40 min). The collected fractions were lyophilized to give a white powder (16 mg, 64%). ^{1}H NMR (600 MHz, DMSO-d_6) δ 1.19–1.39 (m, 30H), 1.43–1.51 (m, 21H), 1.58–1.64 (m, 3H), 2.01–2.05 (m, 10H), 2.09–2.12 (m, 2H), 2.18 (t, 2H, J = 7.4 Hz), 2.58 (d, 1H, J = 12.4 Hz), 2.73–2.77 (m, 4H), 2.82 (dd, 1H, J = 5.1, 12.5 Hz), 2.97–3.06 (m, 12H), 3.08–3.11 (m, 1H), 4.12–4.22 (m, 3H), 4.31 (dd, 1H, J = 5.1, 7.5 Hz), 6.38 (s, 1H), 6.43 (s, 1H), 7.66–7.69 (m, 5H), 7.72–7.75 (m, 4H), 7.87–7.89 (m, 2H), 7.95 (d, 1H, J = 7.7 Hz); HRMS (TOF): *m*/*z* 1179.7860 ($M+H^+$) (calcd for $C_{58}H_{107}N_{12}O_{11}S$: 1179.7903).

4.5. Tubulin binding assay

Fluorescence spectra were measured at 37 °C as described previously.[16] Porcine tubulin (0.5 μM) in MES buffer (0.1 M MES, 0.5 mM $MgCl_2$, 1 mM EGTA, 1 mM GTP, pH 6.8) was incubated with different concentrations of the test compounds (0–12 μM, 1% DMSO) at 37 °C for 1 h. After incubation, the fluorescence of each solution was measured (excitation at 295 nm, emission at 300–450 nm) by FP-750 Spectrofluorometer (JASCO, JAPAN).

4.6. Cell culture

HT-1080 cells were maintained in DMEM medium (high glucose, Wako) containing 10% fetal bovine serum supplemented with 4 mM L-glutamine, 1% PMS at 37 °C in a humidified 5% CO_2 atmosphere.

4.7. Affinity binding of compound 4 (KPU-244-B3) using whole cell lysate

Cell lysate from HT-1080 cells was prepared by rinsing cells in PBS followed by scraping the cells into PBS. The cells were centrifuged and the supernatant was removed. The precipitate was ground in lysis buffer (PBS containing inhibitor cocktail (Roche) and 0.1% NP-40) by using the Plus One Sample Grinding Kit (GE healthcare) and the mixture was then centrifuged at 4 °C. Cell lysate was obtained by transferring its supernatant to another tube and pre-cleaning the supernatant with streptavidin beads (Magna Bind Streptavidin Beads, PIERCE) to remove non-specific proteins. After incubation of the pre-cleaned lysate with compound **4** conjugated streptavidin beads overnight at 4 °C, the beads were washed with lysis buffer four times. The beads were treated with boiling 1× Laemmli's SDS sample buffer (50 mM Tris–HCl (pH 6.8), 2% SDS, 10% glycerol, 0.06% β-mercaptoethanol and 0.02% bromophenol blue) for 5 min to elute proteins retained on the beads. The eluted proteins were then separated by SDS–PAGE using 10% gels. The gels were transferred to a PVDF membrane and blocked with 5% (w/v) skim milk in PBS-T. For detection of α-tubulin, β-tubulin, and β-actin, TU-01 (11-250-C100, EXBIO), tubulin beta (RB-9249-P0, Thermo), and ACTB monoclonal antibody (clone 3G4-F9, Abnova) were used as primary antibodies, respectively.

4.8. Tubulin photoaffinity labeling

Tubulin photoaffinity labeling using KPU-244-B3 was performed using previously described procedures.[16] Briefly, a solution of each compound was added to a tubulin solution (2 μM) in MES buffer (pH 6.8) containing 1 mM GTP and 2% DMSO, and the solution was incubated at 37 °C for 30 min, followed by UV irradiation at 365 nm at a distance of 10 cm on ice for an appropriate time using a UV irradiator (model L9588-01; Hamamatsu Photonics, Hamamatsu, Japan).

4.9. SDS–PAGE, Western blotting

SDS–PAGE and Western Blotting of photolabeled tubulin were performed as previously described.[16] Photolabeled tubulin was separated by SDS–PAGE in 7.5% polyacrylamide gels and transferred to nitro-cellulose membrane. To detect photolabeled protein, the membrane was incubated with streptavidin-horseradish peroxidase conjugate (GE healthcare) for 1 h at room temperature. To detect α-tubulin or β-tubulin, the immunoactive bands were visualized as described above.

4.10. Molecular dynamics simulation of a tubulin binding model

Calculations were performed using Molecular Operating Environment modeling package (MOE 2008.10, Chemical Computing Group, Inc., Montreal, Canada) with MMFF94x force field. Tubulin proteins (chains A and B) were exploited from crystallographic data in complex with colchicine (PDB ID, 1SA0). Compound **2** (KPU-244) binding areas were searched around the tubulin dimer without colchicine using a Site Finder routine implemented in MOE. Compound **2** was docked between the tubulin chains and colchicine binding site. A conformation with high docking scores (interaction energy and superposition on alpha sites) and consistent with experimental results (colchicine competition and possible extension from the benzophenone moiety) was chosen. The binding area was immersed in a 20 Å sphere of TIP3P water molecules centered from the ligand. Compound **2**, contacted residues, and surrounded water molecules were energy-minimized while the other atoms were fixed. Molecular dynamic simulations were performed without heating at 310 K for 300 ps equilibration with 1.5 fs time step. The data were collected at an additional 50 ps of the simulation. Figures were generated using *MacPyMOL* (DeLano Scientific LLC, CA, USA).

Acknowledgments

This research was supported by grants from MEXT (Ministry of Education, Culture, Sports, Science and Technology), Japan, including the Grant-in Aid for Young Scientists (B) 21790118 and the Grant-in Aid for Scientific Research (B) 20390036. We are grateful to Prof. M. Nomizu, Dr. Y. Kikkawa and Dr. K. Hozumi, Tokyo University of Pharmacy and Life Sciences, who provided HT-1080 and gave helpful suggestions. We also thank Prof. Y. Sida, Dr. C. Sakuma, Tokyo University of Pharmacy and Life Sciences for mass spectra and NMR measurements and Dr. J.-T. Nguyen, Kyoto Pharmaceutical University for his manuscript revision.

Supplementary data

Supplementary data associated with this article can be found, in the online version, at doi:10.1016/j.bmc.2010.03.037.

References and notes

1. Desai, A.; Mitchison, T. J. *Annu. Rev. Cell Dev. Biol.* **1997**, *13*, 83.
2. Jordan, M. A.; Wilson, L. *Nat. Rev. Cancer* **2004**, *4*, 253.
3. Zhou, J.; Giannakakou, P. *Curr. Med. Chem. Anti-Cancer Agents* **2005**, *5*, 65.
4. Ferlini, C.; Ojima, I.; Distefano, M.; Gallo, D.; Riva, A.; Morazzoni, P.; Bombardelli, E.; Mancuso, S.; Scambia, G. *Curr. Med. Chem. Anti-Cancer Agents* **2003**, *3*, 133.
5. Skwarczynski, M.; Hayashi, Y.; Kiso, Y. *J. Med. Chem.* **2006**, *49*, 7253.
6. Yusuf, R. Z.; Duan, Z.; Lamendola, D. E.; Penson, R. T.; Seiden, M. V. *Curr. Cancer Drug Targets* **2003**, *3*, 1.
7. (a) Tozer, G. M.; Kanthou, C.; Baguley, B. C. *Nat. Rev. Cancer* **2005**, *5*, 423; (b) Beutler, J. A.; Hamel, E.; Vlietinck, A. J.; Haemers, A.; Rajan, P.; Roitman, J. N.; Cardellina, J. H., II; Boyd, M. R. *J. Med. Chem.* **1998**, *41*, 2333.
8. Sackett, D. L. *Pharmacol. Ther.* **1993**, *59*, 163.
9. Kanoh, K.; Kohno, S.; Asari, T.; Harada, T.; Katada, J.; Muramatsu, M.; Kawashima, H.; Sekiya, H.; Uno, I. *Bioorg. Med. Chem. Lett.* **1997**, *7*, 2847.
10. Kanoh, K.; Kohno, S.; Katada, J.; Takahashi, J.; Uno, I. *J. Antibiot.* **1999**, *52*, 134.
11. (a) Kanoh, K.; Kohno, S.; Katada, J.; Hayashi, Y.; Muramatsu, M.; Uno, I. *Biosci. Biotechnol. Biochem.* **1999**, *63*, 1130; (b) Kanoh, K.; Kohno, S.; Katada, J.; Takahashi, J.; Uno, I.; Hayashi, Y. *Bioorg. Med. Chem.* **1999**, *7*, 1451.
12. Hayashi, Y.; Orikasa, S.; Tanaka, K.; Kanoh, K.; Kiso, Y. *J. Org. Chem.* **2000**, *65*, 8402.
13. Nicholson, B.; Lloyd, G. K.; Miller, B. R.; Palladino, M. A.; Kiso, Y.; Hayashi, Y.; Neulteboom, S. T. C. *Anti-Cancer Drugs* **2006**, *17*, 25.
14. Siemann, D. W.; Bibby, M. C.; Dark, G. G.; Dicker, A. P.; Eskens, F. A. L. M.; Horsman, M. R.; Marme, D.; LoRusso, P. M. *Clin. Cancer Res.* **2005**, *416*, 416.
15. Gaya, A. M.; Rustin, G. J. S. *Clin. Oncol.* **2005**, *17*, 277.
16. Yamazaki, Y.; Kohno, K.; Yasui, H.; Kiso, Y.; Akamatsu, M.; Nicholson, B.; Deyanat-Yazdi, G.; Neuteboom, S.; Potts, B.; Lloyd, G. K.; Hayashi, Y. *ChemBioChem* **2008**, *18*, 3074.
17. Sato, S.; Kwon, Y.; Kamisuki, S.; Srivastava, N.; Mao, Q.; Kawagoe, Y.; Uesugi, M. *J. Am. Chem. Soc.* **2007**, *129*, 873.
18. Saito, S. *Prog. Mol. Subcell. Biol.* **2009**, *46*, 187.
19. Nunes, M.; Kaplan, J.; Wooters, J.; Hari, M.; Minnick, A. A., Jr.; May, M. K.; Shi, C.; Musto, S.; Beyer, C.; Krishnamurthy, G.; Qiu, Y.; Loganzo, F.; Ayral-Kaloustian, S.; Zask, A.; Greenberger, L. M. *Biochemistry* **2005**, *44*, 6844.
20. (a) Dorman, G.; Prestwich, G. D. *Trends Biotechnol.* **2000**, *18*, 64; (b) Dorman, G.; Prestwich, G. D. *Biochemistry* **1994**, *33*, 5661.
21. (a) Vodovozova, E. L. *Biochemistry (Moscow)* **2007**, *72*, 1; (b) Rihakova, L.; Deraet, M.; Auger-Messier, M.; Perodin, J.; Boucard, A. A.; Guillemette, G.; Leduc, R.; Lavigne, P.; Escher, E. *J. Recept. Signal Transduct. Res.* **2002**, *22*, 297.
22. Hayashi, Y.; Katada, J.; Sato, Y.; Igarashi, K.; Takiguchi, Y.; Harada, T.; Muramatsu, M.; Yasuda, E.; Uno, I. *Bioorg. Med. Chem.* **1998**, *6*, 355.
23. Alexopoulos, K.; Panagiotopoulos, D.; Mavromoustakos, T.; Fatseas, P.; Paredes-Carbajal, M. C.; Mascher, D.; Mihailescu, S.; Matsoukas, J. *J. Med. Chem.* **2001**, *44*, 328.